


Effects of Fu's subcutaneous needling on mitochondrial structure and function in rats with sciatica

Molecular Pain
Volume 18: 1–12
© The Author(s) 2022
Article reuse guidelines:
sagepub.com/journals-permissions
DOI: 10.1177/17448069221108717
journals.sagepub.com/home/mpx


Yaping Li¹, Xianghui Gao², Hailiang Huang³, Xiyan Zhou⁴, Yunhua Zang^{4,†}, and Li-Wei Chou^{5,6,7,†} 

Abstract

To observe the effects of Fu's subcutaneous needling (FSN) and acupuncture treatment on the mitochondrial structure and function of the skeletal muscle tissue of rats with sciatica. Forty Sprague–Dawley rats were divided into control, model, acupuncture, and FSN groups (10 each) according to a random number table. The control group was left untreated. Rats in the FSN group were treated with FSN once every 2 days for three times, respectively (days 1, 3, 5, and 7), to cooperate with reperfusion approach. The acupuncture group was treated at the same timeline as that of the FSN group. Changes in the mechanical pain threshold, mitochondrial ultrastructure, mitochondrial citrate synthase (CS) activities, mitochondrial respiratory chain complex II, and mitochondrial COX- I protein expression in the skeletal muscle of rats treated with different treatments were compared with those of the model group. The pain thresholds of the rats were remarkably higher after FSN treatment and acupuncture, and the pain threshold of the FSN group was higher than that of the acupuncture group. Compared with the control group, the mitochondria of the model group had a damaged ultrastructure, were arranged in a disorganized manner, accumulated under the basement membrane, and appeared vacuolated with autophagosomes. The state of mitochondria in the FSN group was close to that in the control group and was remarkably better than that in the acupuncture group. The activities of mitochondrial CS and respiratory chain complex II in the skeletal muscle of the treated rats decreased compared with the control group ($p < 0.05$), and their levels were better in the FSN group than in the acupuncture group ($p < 0.05$). FSN treatment for 1 week considerably improved the pain thresholds and improved the skeletal muscle mitochondrial ultrastructure and mitochondrial function in rats with sciatica.

Keywords

Mitochondrial structure, acupuncture, fu's subcutaneous needling, sciatica, skeletal muscle, tightened muscle, pain

¹Department of Integrated traditional Chinese and Western medicine, Weifang Medical College, Weifang, China

²Department of Integrated traditional Chinese and Western medicine, Huangdaoren Shengtang clinic, Qingdao, China

³Department of Rehabilitation Medicine, Shandong University of Traditional Chinese Medicine, Jinan, China

⁴Department of Neurology, Qingdao Hospital of Traditional Chinese Medicine (Qingdao Hiser Hospital), Qingdao, China

⁵Department of Physical Medicine and Rehabilitation, China Medical University Hospital, Taichung, Taiwan

⁶Department of Physical Therapy and Graduate Institute of Rehabilitation Science, China Medical University, Taichung, Taiwan

⁷Department of physical Medicine and Rehabilitation, Asia University Hospital, Asia University, Taichung, Taiwan

[†]Yunhua Zang and Li-Wei Chou contributed equally to this work.

Corresponding Author:

Li-Wei Chou, Department of Physical Medicine and Rehabilitation, China Medical University Hospital, No 2 Yuh-Der Road, Taichung, 404332, Taiwan.
Email: chouliwei@gmail.com



Creative Commons Non Commercial CC BY-NC: This article is distributed under the terms of the Creative Commons Attribution-NonCommercial 4.0 License (<https://creativecommons.org/licenses/by-nc/4.0/>) which permits non-commercial use, reproduction and distribution of the work without further permission provided the original work is attributed as specified on the SAGE and

Open Access pages (<https://us.sagepub.com/en-us/nam/open-access-at-sage>).

Introduction

Fu's subcutaneous needling (FSN) was invented by Dr. Zhonghua Fu in 1996. Dr. Fu integrated modern anatomy, sports medicine, physiology, biomechanics, and fasciology in developing a special field of medicine for more than 20 years; he formed FSN's characteristic theoretical system and clinical diagnosis and treatment patterns.¹⁻³ FSN therapy is widely used, and its efficacy is exact for somatic and visceral pain; it also has remarkable effects on non-painful conditions, such as chronic bronchitis, stress urinary incontinence, chronic superficial gastritis disease, Parkinson's disease, myopia, and intractable diarrhea, but its specific mechanism of action is yet to be elucidated.⁴⁻⁶ The diseases that FSN can treat, including painful or non-painful diseases, are initially caused by muscle problems. Long-term muscle overload, exercise, incorrect force posture, and muscle atrophy and degeneration lead to ischemia and hypoxia of muscle tissues and cause myofascial trigger point (MTrP) via the theory of energy crisis.⁷ FSN acts on connective tissues that are closely related to muscles, particularly tightened muscles (TMs), as proposed by Dr. Zhonghua Fu in 2014. TMs are muscles with a single or multiple MTrPs and present as tightness and cramps when the central nervous system is relaxed but the target muscle is fully or partially stiff because of ischemia or hypoxia in local muscle tissues.⁸

In 2011, the International Pain Association defined neuropathic pain as a chronic pain caused by nerve injury. Sciatica belongs to neuropathic pain, including primary and secondary pain. Intervertebral disc herniation is the most common cause of sciatica. Other causes include the inflammatory material exudation of muscle injury, intraspinal tumor, and lumbar spinal stenosis⁹ as well as sacroiliac arthritis, pelvic tumors, and diabetes. Clinically, acupuncture and FSN can improve the clinical symptoms of sciatica. Many clinical studies have shown that the overall efficacy of acupuncture, including electroacupuncture, warm acupuncture, and FSN, is better than that of conventional Western medicine therapy, and acupuncture can effectively reduce pain symptoms and improve the quality of life of patients without any toxic and side effects.¹⁰⁻¹¹ Whether the good effects of FSN or acupuncture is exerted through subcutaneous connective tissues and muscle tissues still needs to be explored. Muscles have nutritious and innervated nerves. Muscle denervation and innervated nerve apoptosis occur following nerve injury. In the absence of nerve activity, muscle will atrophy; muscle mass will be reduced; and muscle strength, fiber diameter and quantity will be reduced in varying degrees.¹²⁻¹⁴ Although sciatic nerve injury belongs to peripheral neuropathy, relevant literature reported that ligating the sciatic nerve will induce severe pain and lead to the atrophy of related muscles.¹⁵ Therefore, FSN is hoped to be used to treat the injured nerve and muscle tissue, improve mitochondrial function, and prevent muscle atrophy.

Materials and methods

Experimental animals and grouping

Forty rats (specific pathogen-free grade, body weight 250 ± 10.5 g, aged 7 weeks) were purchased from Ponyue Animal Center, Jinan, China. The rats were caged, given standard rat chow and water, and housed in the laboratory animal center of Wei Fang Medical College with the approval of the ethics committee of Wei Fang Animal Medical Center (SCXK(鲁)20190003). The environment was kept at a constant temperature of 25°C, a relative humidity of 40%–70%, and a 12-h light/dark cycle. The rats were adaptively housed for 7 days and divided into four groups using a random number table method with SPSS: Control (COT) group, Model (MOD) group, acupuncture (ACP) group, and FSN group (Figure 1).

Main instruments and reagents

The instruments used include a horizontal decolorization shaker (Beijing Dingguo Biotechnology Co, Ltd.), an ultrapure water machine (Shanghai Hetai Instruments Co., Ltd.), a low-temperature high-speed centrifuge (Eppendorf, Germany), a pipette (Biosharp, China), a -80°C cryogenic refrigerator (Japan), a transmission electron microscope (JEM-1400, Japan), a special imaging system for transmission electron microscope (Gatan, USA), a microplate reader (BioRad, USA), an electrophoresis apparatus (BioRad, USA), an electrophoresis tank (BioRad, USA), and a gel imaging system (BioRad, USA). The BCA Protein Quantification Kit, Animal Tissue Mitochondria Isolation Kit, Rat Citrate Synthase (CS) Enzyme-linked Immunosorbent Assay (ELISA) Kit, and Respiratory Chain Complex II ELISA Kit were purchased from Beyotime Institute of Biotechnology, Shanghai, China. Anti-GAPDH and anti-Cox I were from Abcam (Nanjing).

Modeling method

Bennet et al. established a sciatic nerve model with chronic constriction injury (CCI) in 1988.¹⁶ The rats were placed prone on the operating table. The right hind limb was shaved and disinfected. The leg skin was cut, the subcutaneous fat and superficial fascia were separated layer by layer, and the biceps femoris was passively separated with ophthalmic forceps with both hands to expose the sciatic nerve trunk. The sciatic nerve trunk was picked out with a glass minute needle and ligated four times with a spacing of about 1 mm. The ligation force should not affect the blood transport of the nerve adventitia (4-0 medical catgut was used as the ligation line), and a slight twitch of the limbs was observed during ligation. After ligation, the muscle and skin were sutured layer by layer, and penicillin sodium powder was applied to the wound before and after suturing to prevent infection¹⁶ (Figure 2). The control group was not operated. The other

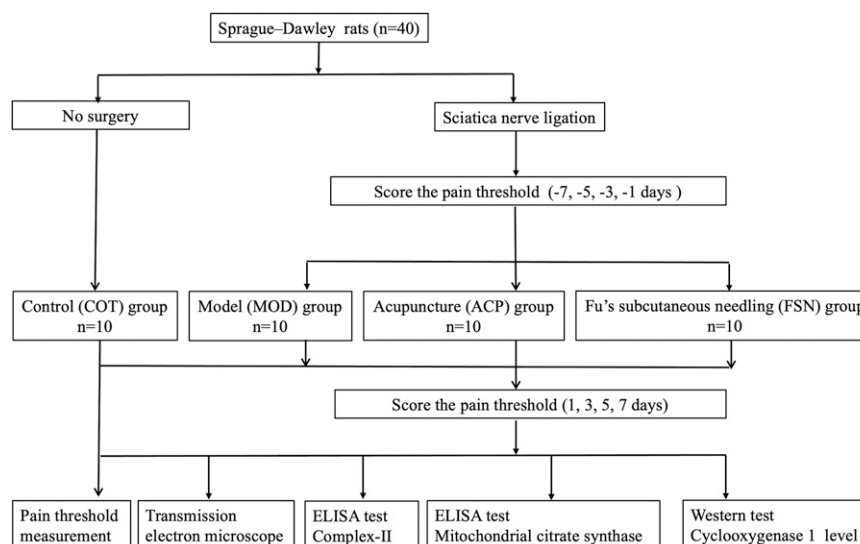


Figure 1. Flow chart of animal experiment.

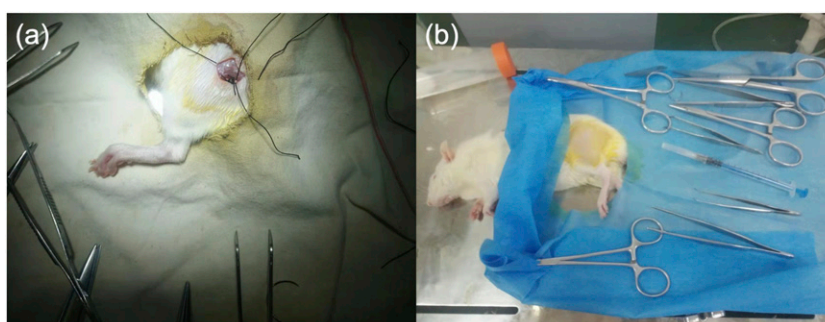


Figure 2. (a) 4-0 medical catgut was used to ligate the sciatic nerve and four knots. (b) Anesthetized rat was fixation for skin preparation and posterolateral thigh surgery.

three groups were divided according to the rat model of sciatica, and then the sciatic nerve was double ligated to establish the chronic injury model. After modeling, the pain threshold was measured on days 1, 3, 5, and 7. Neuropathic pain appears indicates that the modeling was successful, and the unsuccessful rats were excluded. The intervention began on day 1. (Figure 3)

Treatment protocol

After modeling, the ACP and FSN groups were treated. The rats were fixed and disinfected prior to treatment. The ACP group was treated with acupuncture. Rats were acupunctured with 1.25 mm-diameter needles in two acupoints: "Wei-zhong (BL40)", and "Huan-tiao (GB30)" (Figure 4(b)) without anesthetization. The location of "Wei-zhong (BL40)" was on the depression in the posterior square of the knee joint of the hind limb and "Huan-tiao (GB30)" was on the posterior upper

edge of the hip joint of the hind limb.¹⁷ After the rats in the ACP group were fixed with the rat fixator, the needles were kept for 20 min after the needle entered the acupoints. During this period, we observed the situation of the rats and whether the needle fell. If the needle fell, acupuncture was performed again.

The FSN group was treated with FSN disposable needle (Nanjing paifu). (Figure 4(a)). The FSN needle was inserted toward the TM (the needle entry position was approximately near the gluteus maximus muscle). The needle was rapidly advanced to prevent the rat from being tense, which causes the muscle to contract and hinder the entry of the needle. Once the needle entered the skin, the needle was swayed, and the reperfusion approach was performed. The swaying movement, a key procedure for FSN, is a smooth, soft, fan-style waggle that uses the thumb as the fulcrum. The index, middle, and ring fingers stay in a line. The middle finger and thumb affix the needle in a face-to-face way, whereas the

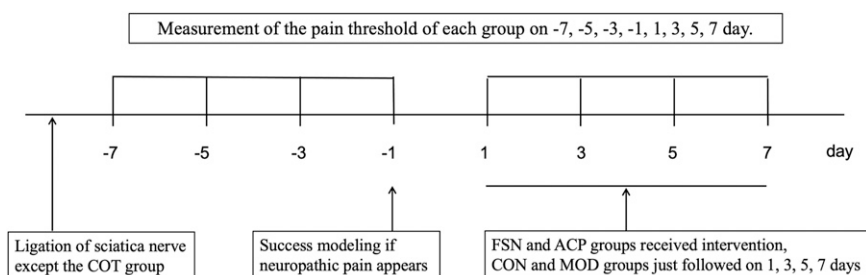


Figure 3. Time flowchart of this study. Before modeling, the pain threshold of rats of each group was measured as an initial threshold. Since the first day (-7) after modeling, the pain threshold in each group was measured, and followed by every 2 days respectively (-5, -3, -1, 1, 3, 5, 7) days. The pain threshold measured on "-1" day indicated that the modeling was successful. After the completion of modeling, the intervention started on "1" day. Except for the COT and MOD group, the FSN and ACP group were treated with FSN needle and acupuncture at fixed time points on (1, 3, 5, 7) days respectively. FSN: Fu's subcutaneous needling; ACP: acupuncture; MOD: model; COT: control.

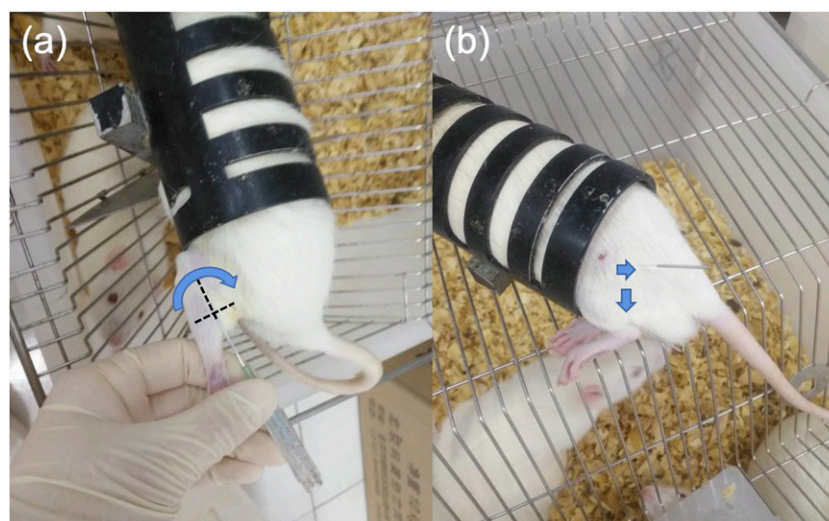


Figure 4. The rats were fixed and received intervention without anesthesia. (a) Fu's subcutaneous needling (FSN) with the needle tip toward the gluteus maximus muscle was manipulated as the swaying movement (blue fan) in FSN group. (b) Acupuncture (ACP) was needled on "Huan-tiao (GB30)" and "Wei-zhong (BL40)" points (blue arrows) in ACP group.

index and ring fingers alternately move back and forth. The FSN group was treated with a FSN needle with both hands combined with swaying and reperfusion approach. The frequency was 100 times/min, and the operation was about 1 min. The manipulation was performed once every 2 days for four times (days 1, 3, 5 and 7). The ACP group was treated the same time as the FSN group.

Sampling and sample preparation

1. Electron microscopy sample preparation: The rats were weighed in batches and anesthetized by intraperitoneal injection with 3% pentobarbital (30 mg/kg). A blade was used to rapidly separate a small piece of rat pear Longus longitudinally along the muscle fiber into $2 \times 1 \times 1 \text{ mm}^3$ and then pre-chilled in 2.5% glutaraldehyde at 4°C for electron microscopy.

2. Preparation of skeletal muscle mitochondria: Each muscle tissue sample (100 mg) was placed in a pre-chilled lysis solution and analyzed using the Beyotime Animal Tissue Mitochondria Isolation Kit.

Index and methods

1. Measurement of mechanical pain threshold: The pain threshold was measured every 2 days. The rats with a confirmed group and number were placed in a box on a metal net with six rats each. Wait for 15–30 min until the rats keep quiet in the strange environment (do not walk around the cage or the rats will lick themselves). According to the pre-experiment, the von Frey hair values of 4, 6, 8, 10, 15, 26, 60, and 100 g were used for measurement. When measuring, the middle value (10 g) should be set as the starting point, and the values

were measured in ascending order. When crossing for the first time, measure the values four times. Von Frey hair acts on the bottom of the toe between the left foot pads of rats. This position has a moderate response to mechanical stimulation and can directly reflect the degree of neuralgia.¹⁸ Handheld von Frey hair had an "S" shape, the action time was 6–8 s, and the interval between adjacent stimuli was at least 7 s. A reaction was considered a positive reaction if the rats lift their feet or lick the stimulated side during the action time. In the stimulation process, rat movements, such as moving around or lifting their feet, upon stimulation are considered suspicious; therefore, the measurements were carried out after the rats calm down. The positive result was recorded as X, and the negative was O. The measurement results were recorded. The calculation formula is $50\% g \text{ (threshold)} = (10^{[X_f + K\delta]})/10,000$, where X_f is the logarithm of the number of g corresponding to the last measurement, and the corresponding log units were 4.56, 4.74, 4.93, 5.07, 5.18, 5.46, 5.88, and 6.1 respectively, put in the final formula. (Calculation method: Log(corresponding to 10,000×g)), the value of K comes from the table lookup, and its calculation formula is $\delta = 0.22$ (select the average value of the difference between two adjacent values of log unit sequence) the final result obtained by the formula is the g number.

2. Transmission electron microscopy (TEM): The rat piriform muscle was rapidly isolated, and the surrounding muscle was removed with a blade. The samples were rinsed three times with 0.1 M pre-chilled PBS and then overnight at 4°C. Osmium (1%) was added the following day for 2 h fixation at 4°C. The slides were washed sequentially with a concentration gradient of 50%, 70%, and 90% ethanol; 90% ethanol:90% acetone 1:1, 90% acetone, and anhydrous acetone (three times) The dehydration time was 15 min. Briefly, anhydrous acetone was immersed with the embedding agent according to the following formula: 3:1, 1:1, and 1:3. Then, the pure embedding agent, was added by shaking for 30 min. Finally, the pure embedding agent was immersed overnight. The next day, the immersed samples were placed in an embedding plate into which the embedding agent was injected and polymerized, and the polymerization temperature was set to 37°C for 12 h, 45°C for 12 h, and 60°C for 24 h. The samples were embedding with epoxy resin (Spurr), cut longitudinally, made into ultra-thin sections and stained with acetic acid di-oxygen axis and lead citrate. After the samples were dried, the mitochondrial ultrastructures were observed by TEM. Each tissue section was observed first in the low power field of view (500–1000×) and then in the high power field of view (20,000–

50,000×) to observe the distribution, size, morphology, crista structure, and autophagosome formation of the mitochondria.

3. The mitochondrial CS content and respiratory chain complex II in gluteus maximus muscle were measured by ELISA. The specific procedures were performed according to the kit procedures.
4. Western blot analysis. The COX-I protein content of the gluteus maximus muscle was determined by Western blot. Briefly, small pieces of gluteus maximus muscle were reduced in pre-chilled lysis buffer and homogenized by a homogenizer, centrifuged at 12,000×g for 10 min at 4°C, and finally boiled for 5 min at 98°C. The sample was stored at –20°C for future use.

Data statistics and processing

The data were analyzed by GraphPad Prism statistical software. The data were expressed as mean ± standard deviation. Two-way ANOVA was used to analyze the main effects of processing factors and sampling time factors and their interaction. The statistical method of individual effects among groups was analyzed by one-way ANOVA. If the variance was homogeneous, the SNK-q method was used. If the variance was not homogeneous, the original data was converted to become homogeneous before statistical analysis. For the index data that cannot be converted, the statistical results of Tamhane's T2 were directly used for analysis. $p < 0.05$ was statistically significant.

Results

Changes in the mechanical pain threshold of rats

The pain thresholds of rats were measured at different time points after modeling, and the pain thresholds were expressed by mean ± SD (Table 1).

The experimental results showed that except the CON group, no significant difference in pain threshold was found between the other groups at days -7, -5, -3, and -1 days after the completion of modeling. From the first day after the intervention, the pain threshold of the MOD, FSN, and ACP groups changed considerably. After the intervention, the pain threshold of the FSN and ACP groups increased in varying degrees from the third day, and the pain threshold of the FSN group was higher than that of the ACP group ($p < 0.05$). From the first day, the pain threshold of the model group without any intervention still decreased in varying degrees, but the pain threshold of the FSN and ACP groups were higher than that of the MOD group in varying degrees ($p < 0.05$ between the FSN and MOD group, $p < 0.05$ between the ACP and MOD groups) (Figure 5).

Table 1. Changes of mechanical pain threshold in each group.

Timeline	COT group	MOD group	ACP group	FSN group
-7	32.1 ± 2.1	33.5 ± 4.7	34.7 ± 3.6	33.7 ± 5.6
-5	31.6 ± 2.3	34.2 ± 3.7	33.1 ± 4.7	34.1 ± 4.0
-3	31.3 ± 3.0	32.8 ± 2.8	34.7 ± 3.3	32.1 ± 3.5
-1	32.8 ± 3.3	21.3 ± 3.3	22.1 ± 4.8	21.3 ± 5.1
1	34.2 ± 2.7	19.6 ± 2.2	19.9 ± 2.8	20.1 ± 3.7
3	33.3 ± 2.6	15.0 ± 3.1* [▲]	22.6 ± 2.1*	22.8 ± 3.8* [#]
5	32.6 ± 3.7	13.7 ± 4.5* [▲]	23.7 ± 3.6*	27.7 ± 4.9* [#]
7	34.4 ± 2.9	15.6 ± 3.7* [▲]	25.1 ± 2.9*	29.3 ± 2.8* [#]

Data were expressed as mean ± SD; *p* value was analyzed by One way ANOVA FSN: Fu's subcutaneous needling; ACP: acupuncture; MOD: model; COT: control;

Timeline -7, -5, -3, -1 represent the first, third, fifth, seventh days after nerve ligation; Timeline 1, 3, 5, seven represent the first, third, fifth, seventh days of intervention in each group. FSN group and ACP group compared with the MOD group: *P** < 0.05; FSN group compared with the ACP group: *P*[#] < 0.05; MOD group compared with the COT group: *P*[▲] < 0.05.

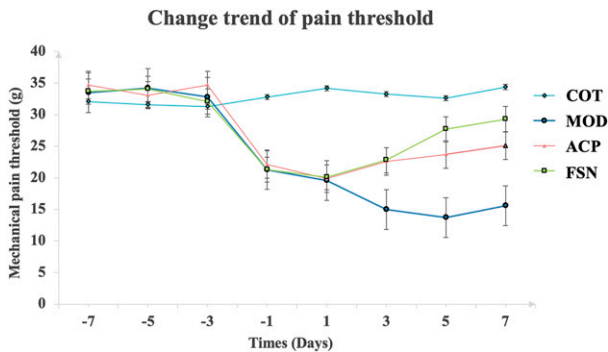


Figure 5. Change trend of pain threshold of rats in each group. FSN: Fu's subcutaneous needling; ACP: acupuncture; MOD: model; COT: control.

Changes in the mitochondrial ultrastructure of the gluteus maximus muscle of rats in each group

In this study, TEM was used to observe the changes in the mitochondrial ultrastructure of rats with sciatica using different intervention maneuvers. Under an electron microscope, the myofibril structure of the COT group was clear and complete, the mitochondria were orderly arranged, the mitochondria were long strip or oval, the bilayer membrane structure was complete and clear, the ridge structure was full and dense, and no obvious phagosomes was found (Figure 6 a1, a2). Remarkable differences in the mitochondrial ultrastructure among the MOD, ACP, and FSN groups after successful modeling before any interventions. Compared with the COT group, the arrangement of the mitochondria in the MOD group was disordered, the Z-line was partially broken, the number of mitochondria was remarkably reduced, and no obvious vacuolized structure and autophagy were

found (Figure 6 b1, b2). One week after ACP treatment, the mitochondrial structure was observed under an electron microscope. Some mitochondria of skeletal muscles were still unevenly distributed. The mitochondria existed under the muscle membrane; the morphology of the mitochondria was irregular; and the mitochondria became larger, swollen, and vacuolized with unclear ridge structure and autophagic vesicles (Figure 6 c1, c2). After treatment with FSN, the mitochondrial structure of the model rats was remarkably restored compared with those of the MOD and ACP groups. The morphology of the mitochondria was regular; the structure was clear; and a few swelling, deformation, and vacuolization of the mitochondria occurred (Figure 6 d1, d2).

Mitochondrial CS content

Mitochondrial CS is a quantitative enzyme that reflects the number of complete mitochondria in tissues.¹⁹ It is one of the three rate-limiting enzymes of the tricarboxylic acid cycle. It is exchanged and replaced in normal muscle. Studies have reported that after the ligation of the sciatic nerve, the activities of related enzymes in the skeletal muscles' mitochondria decreased in varying degrees, such as the levels of cytochrome C oxidase, succinate dehydrogenase, CS, and glycine synthase.^{12,20-21} The experimental results showed that the gluteus maximus muscle of rats was damaged in varying degrees and the mitochondria were damaged. Different intervention methods had different effects on the expression of mitochondrial CS in the gluteus maximus muscle of rats CS in rat skeletal muscle was significantly higher in the FSN and ACP groups than that in the model group (*P** < 0.05), and the activity of respiratory chain complex in the FSN group was higher than that in the ACP group (*P*[#] < 0.05). A little difference was found between the COT and MOD group (*P*[▲] < 0.05). (Table 2, Figure 7(a))

Mitochondrial respiratory chain complex II content

The CS content in the tricarboxylic acid cycle is often used to standardize the activity of the complex to eliminate the influence of quantitative mitochondrial changes, particularly the mitochondrial respiratory chain complex. The standardized experimental results showed that the activity of the mitochondrial respiratory chain complex II in rat skeletal muscle was significantly higher in the FSN and ACP groups than that in the model group (*P** < 0.05), and the activity of respiratory chain complex in the FSN group was higher than that in the ACP group (*P*[#] < 0.05). A little difference was found between the COT and MOD group (*P*[▲] < 0.05) (Table 2, Figure 7(b))

COX- I protein content in gluteus maximus muscle was determined by Western blot

The experimental results showed that the protein expression of COX- I in the skeletal muscle after different intervention

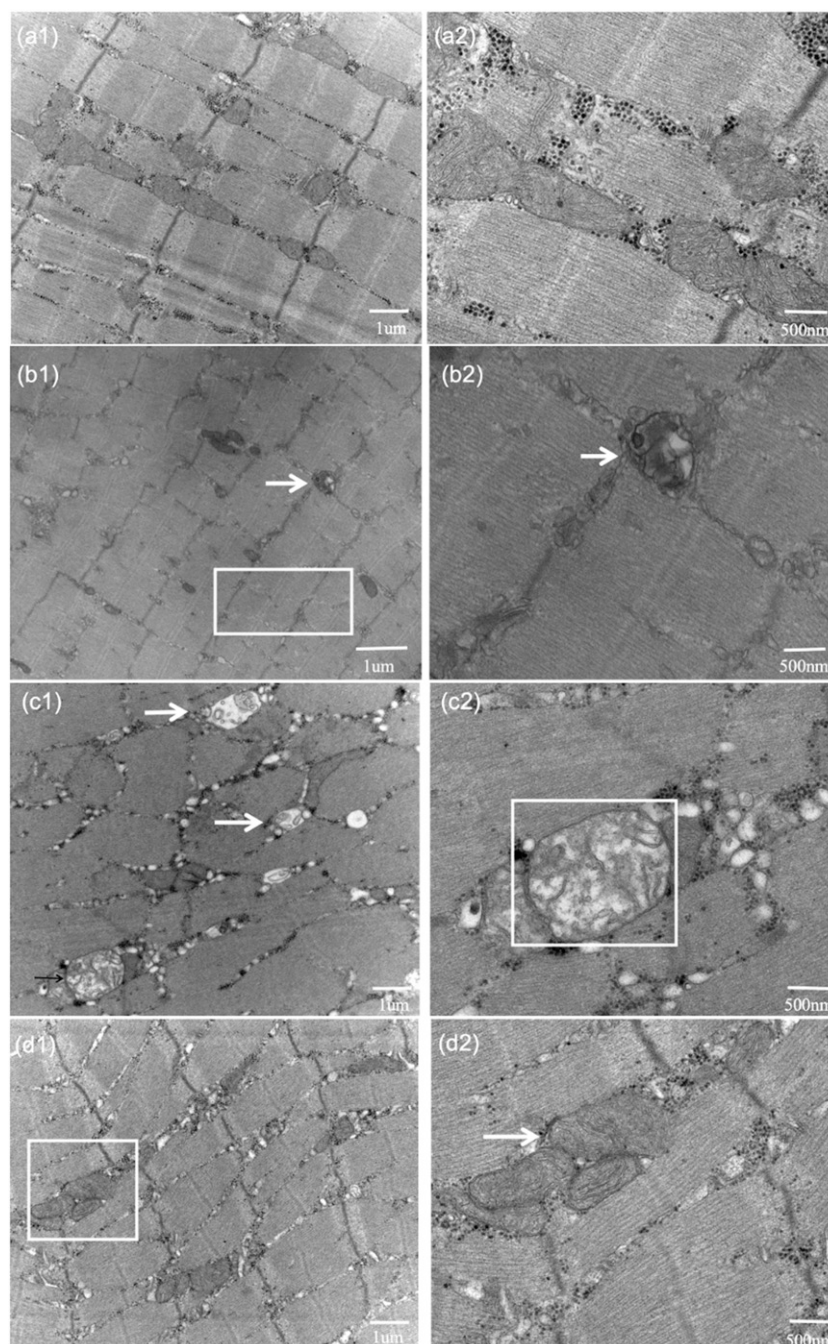


Figure 6. Changes in the mitochondrial ultrastructure of the gluteus maximus muscle of rats in each group under transmission electron microscope. The arrows and box indicated by the arrows in b1 and b2 represented the place where a large number of mitochondria were missing, and the number of mitochondria in tissue decreased. At the places indicated by c1 arrows and c2 box, mitochondria appear vacuolized structure. At the place indicated by d1 box and d2 arrow, the structure of muscle tissue and the morphology of mitochondria were improved. a1, a2: COT group; b1, b2: MOD group; c1, c2: ACP group; d1, d2: FSN group. Observation under 20,000x electron microscope: a1, b1, c1, d1; Observation under 50,000x electron microscope: a2, b2, c2, d2. Dyeing method: acetic acid dioxigen axis, lead citrate. FSN: Fu's subcutaneous needling; ACP: acupuncture; MOD: model; COT: control.

methods was different and showed a downward trend. The protein expression of COX- I decreased after modeling. A remarkable difference in COX- I expression was found between the FSN and ACP groups. The COX- I protein

expression of the FSN group was higher than that of the ACP group ($P^{\#} < 0.05$). The COX- I protein expression in the FSN group was significantly higher than that in the model group ($P^* < 0.05$). Compared with the MOD group, have a

Table 2. Changes in the content of mitochondrial CS, Complex II/CS, and COX- I.

	COT group	MOD group	ACP group	FSN group
CS (ng/ml)	10.08 ± 0.76	7.05 ± 0.39 [▲]	7.79 ± 0.34*	8.66 ± 0.51 [#]
Complex II/CS (ration)	0.92 ± 0.08	0.62 ± 0.64 [▲]	0.66 ± 0.06*	0.81 ± 0.09 [#]
COX- I (ng/ml)	1.22 ± 0.88	0.52 ± 0.19 [▲]	0.57 ± 0.23	1.03 ± 0.80 [#]

Data were expressed as mean ± SD; *p* value was analyzed by One way ANOVA; FSN: Fu's subcutaneous needling; ACP: acupuncture; MOD: model; COT: control; CS: Mitochondrial citrate synthase; Complex II: Mitochondrial respiratory chain complex II; COX- I: Cyclooxygenase I.

FSN group and ACP group compared with the MOD group: *P** < 0.05; FSN group compared with the ACP group: *P*# < 0.05; MOD group compared with the COT group: *P*▲ < 0.05.

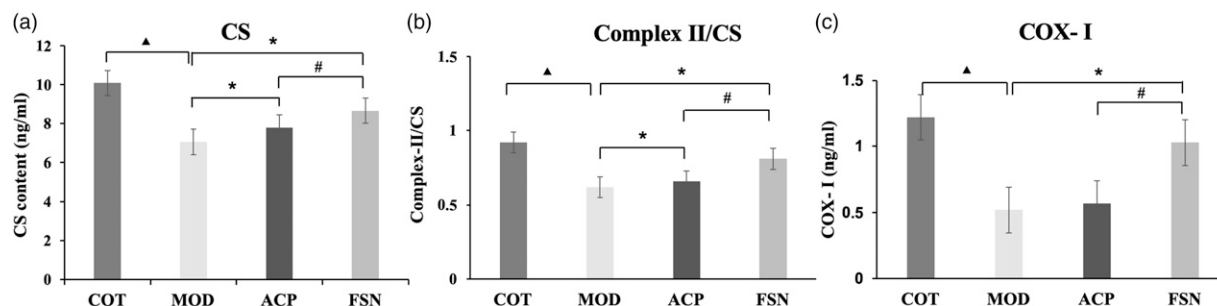


Figure 7. Changes trend of mitochondrial CS content (a), complex II/CS ratio (b) and COX-I protein expression (c) in muscles with different intervention methods. CS: Mitochondrial citrate synthase; Complex II: Mitochondrial respiratory chain complex II; COX- I: Mitochondrial Cyclooxygenase I. FSN: Fu's subcutaneous needling; ACP: acupuncture; MOD: model; COT: control. FSN group and ACP group compared with the MOD group: *P** < 0.05; FSN group compared with the ACP group: *P*# < 0.05. MOD group compared with the COT group: *P*▲ < 0.05.

significant difference in protein expression was found in COT group (*P*▲ < 0.05) (Table 2, Figure 7(c)).

Discussion

A large number of clinical studies has confirmed that FSN can effectively alleviate pain in the treatment of chronic diseases. However, no in-depth study has shown why intervention in connective tissues can improve the state of TM, as well as the possible influencing factors that can change the physical and chemical states of muscles. In this experiment, FSN was applied to the rat model of chronic pain. The specific mechanism of FSN in the treatment of chronic pain was analyzed by observing and comparing the morphological structures of mitochondria in muscle tissues before and after FSN treatment. Some important factors affecting mitochondrial energy metabolism were also analyzed. The experimental results showed that after 1 week of modeling, the number of mitochondria in the TM decreased; the structure and organization were disordered; and the mitochondria were deformed, swollen, and even vacuolized. The muscle tissues and fibers underwent atrophy, Z-line breakage, distortion and other phenomena. After 1 week of FSN treatment, a great degree of mitochondrial regeneration occurred, and the mitochondrial morphology and structure improved compared with the MOD and ACP groups. Compared with the MOD and ACP groups, the pain threshold in the FSN group was remarkably higher, which was similar to the results of another

experiment.²² After a week of FSN treatment, CS and mitochondrial complex II in the mitochondrial structure improved compared with the MOD and ACP groups. The CS contents in the FSN, ACP, and MOD groups were 8.66 ± 0.51 , 7.79 ± 0.34 , and 7.05 ± 0.39 , respectively. The CS content in the FSN group was significantly higher compared with those in the ACP and MOD groups. This key enzyme reflects the activity and intensity of mitochondrial energy metabolism. After FSN treatment, the expression of mitochondrial COX- I protein in the muscle tissue increased. The COX- I protein activities in the FSN, ACP, and MOD groups were 1.03 ± 0.80 , 0.57 ± 0.23 , and 0.52 ± 0.19 . The FSN group had significantly higher COX- I protein than the other two groups. COX- I protein expression is closely related to mitochondrial function and cell energy production. These results have a good response to the effect of FSN on muscles.

After peripheral nerve injury, muscle denervation can lead to skeletal muscle atrophy and inactivation and reduce the contractile and metabolic functions of the skeletal muscle.²² In the CCI rat model, the nutritional function of the corresponding innervated muscle decreases after ligation of sciatic nerve causes nerve damage, and metabolic abnormalities, such as the waste produced by muscle tissue produce energy crisis slowly forms pathological muscles (i.e. TM). Continuous TM causes pain. FSN and acupuncture target the connective tissue, which does not directly act on the damaged nerve and muscle parts but has also produced good results in clinic. In the many clinical neurological diseases, the main

problem lies in the muscle rather than the nerve itself, which is worthy of our discussion. Therefore, in the sciatica rat model, this experiment changed the mitochondrial structures and function of muscles under the treatment of FSN to study the treatment mechanism of FSN for chronic pain diseases. The theory of traditional Chinese medicine and the research of modern histopathology and molecular biology have made great progress, which provides certain conditions for the discussion of the mechanism of FSN therapy. Mechanical connective tissue reaction instead of neural mechanism in FSN treatment was first investigated in a rabbit model on 2012.²³ This hypothesis was also supported in the study via Langevin and her colleagues.²⁴ Fascia theory holds that connective tissues have the functions of connection, nutrition, transportation, and defense but also has the functions of support and reserve. It can repair the body by stimulating fascia connective tissue.²⁵ Previous experiments showed that stimulating the fibers in connective tissue through mechanical traction can restore the disordered connective tissue fibers in the disease state to the arrangement state consistent with the stress direction, but it can also drive changes in cell morphology and cytoskeleton in the reticular scaffold through mechanical traction to transmit the extracellular mechanical signal to the cells. The change in connective tissue cell signal transduction resulted in the change of relevant cytokine concentration, caused the change of cell microenvironment, and finally promoted the body to return to equilibrium.^{26–27} FSN therapy has immediate, short-term and long-term effects on diseases.²⁸

The mitochondria exist in muscles, whereas the FSN acts on connective tissue. When FSN was removed from the animal body, it always does not look so smooth on the needle head, which is similar to something with small debris. An electron microscope study found that when the acupuncture needle was lifted, inserted, and twisted in the human body. The acupuncture needle was removed, and debris was found on the acupuncture needle, revealing that connective tissues, such as elastic fibers and collagen fibers were wound around the needle.²⁸ Connective tissue includes loose connective tissue, such as subcutaneous tissue and dense connective tissue, such as tendon. Connective tissue is generally composed of cells, fibers, and extracellular stroma. In cells, it includes common fibroblasts, adipocytes, and mesenchymal cells, as well as some uncertain macrophages, plasma cells, mast cells, and white blood cells exuded from blood. When the FSN was inserted into the skin, it had an important impact on the connective tissue, which enhanced the mechanical coupling between the needle and the connective tissue. The swaying movement of the FSN and the lifting, inserting, and twisting method of the needle continuously enhance this mechanical coupling. Acupuncture can transmit mechanical signals to connective tissue through this mechanical coupling.²⁴ The downstream effects of mechanical signals may include the synthesis and local release of growth factors, cytokines, vasoactive substances,

degrading enzymes, and structural matrix elements. The release of these substances may affect the extracellular environment around connective tissue cells.²⁹ It may be related to reducing pain. However, at present, little is known about the innervation of connective tissue, and fully explaining why FSN entering the connective tissue can produce a good analgesic effect is impossible. However, fascia, especially extramuscular fascia and aponeurosis fascia, is recently considered a small straight fiber with high innervation, which can transmit nociceptive signals, especially in the presence of inflammation.^{30–32} Determining how much pressure and tension the connective tissue is under to produce a good painless feeling is also difficult. These factors need further study.

As the center of cell energy and material metabolism, the oxidative phosphorylation reaction on the respiratory chain of the mitochondria supplies energy for muscle contraction and other life activities and controls cell survival by producing adenosine triphosphate (ATP), which provides fuel for cell processes. In turn, it induces cell death by releasing pro-apoptotic factors, such as cytochrome C. Its fusion and division are the manifestations of mitochondrial dynamics. Mitochondrial fusion and division are the key to maintain the normal morphological structure and dynamic function of the mitochondria. Fusion and division come first, and apoptosis comes later.³³ Mitochondrial dynamics shapes the morphological structure of the mitochondria, which is closely related to mitochondrial dynamics and affects the metabolism of cell energy and the occurrence of autophagy and apoptosis.³³ The timely removal of damaged mitochondria through mitochondrial autophagy is very important for cell balance and function. The best predictor of mitochondrial content is mitochondrial CS activity, followed by complex I activity and complex II protein content. CS is a marker enzyme that reflects the structural integrity of the mitochondria, and its content directly reflects the number of surviving mitochondria in tissues.³⁴ Mitochondrial complex II, also known as succinate dehydrogenase, is a central provider of metabolic and respiratory adaptation reprogramming. It is a marker enzyme reflecting mitochondrial function. Its activity can be used as an index to evaluate the level of intracellular energy (i.e., ATP synthesis). The present study was found that FSN and acupuncture treatment for rats with chronic pain improved the morphological structure of the mitochondria and the expression of related proteins to a certain extent.

Mitochondrial structural damage and dysfunction have an important impact on the neurological diseases of the central and peripheral nervous systems.³⁵ The role of mitochondrial dysfunction in the pathogenesis of chronic pain is exerted through the five functions of the mitochondria, namely, mitochondrial energy generation system, reactive oxygen species (ROS) generation, mitochondrial permeability transition pore (MPTP), apoptosis pathway, and intracellular calcium mobilization.³⁶ Mitochondrial energy generation system is mainly

completed by tricarboxylic acid cycle and mitochondrial electron transport chain. ATP is produced by enzymes on the electron transport chain through a series of reactions. Enzymes on the mitochondrial respiratory chain are closely related to the generation of pain.³⁷ ROS are generated when electrons in the mitochondrial respiratory chain leak out of the respiratory chain and consume about 2% of oxygen before being transferred to the terminal oxidase. The electron flux in the respiratory chain determines the amount of ROS generated. ROS include highly reactive species, such as hydroxyl radical ($\bullet\text{OH}$), and weakly reactive species, such as superoxide ($\text{O}_2\bullet^-$), which are the by-products of oxidative phosphorylation.^{38–39} To some extent, ROS participate in mitochondrial autophagy, the homeostasis of mitochondrial environment, and signal transduction. However, when the increase in ROS exceeds the antioxidant capacity of the mitochondria, excessive ROS will damage the morphological structure of the mitochondria, endanger cell function, and produce irreversible damage. ROS are also involved in persistent pain.^{39–42} Mitochondrial permeability transition pore (MPTP) is a group of protein complexes existing between the inner and outer membranes of the mitochondria. It is a non-specific channel. MPTP plays an important role in cell survival and apoptosis. It involves many fields, such as ischemia/reperfusion, tumor, aging, and neurodegeneration.⁴³ Mitochondrial permeability transition is closely related to pain. Inhibiting the opening of mitochondrial permeability may contribute to mitochondrial homeostasis. Apoptosis is a kind of programmed cell death, which occurs due to the production of several catabolic enzymes. In this process, some morphological and biochemical changes have taken place in the mitochondria. The mitochondria are the main organelles involved in apoptosis and control the apoptotic pathways in cells.^{44–45} FSN therapy acts on the connective tissue closely related to the muscle tissue. Through the continuous traction of connective tissues, FSN improves the cell and the extracellular environment of connective tissue, and improves the energy system of the muscle tissue (mitochondria) through the transmission of mechanical signals between tissues, which provides a theoretical basis for the FSN therapy of chronic pain diseases, it also provides ideas for the continuous development of FSN in the future.

Conclusion

The use of FSN treatment for chronic pain can improve the morphological structure and function of the mitochondria in the tightened muscle, increase the content of mitochondrial CS and Complex II, increase the active expression of COX- I protein in the muscle tissue, improve muscle energy metabolism, and relieve muscle pain in rats. These effects are related to the signal transduction of the connective tissue and muscle and the release of energy crisis. FSN therapy can remarkably improve this kind of

neuropathic pain and promote the recovery of damaged nerves and muscles.

Author contributions

Yaping Li performed the animal experiment, analyzed the data and wrote the original draft and performed immunoprecipitation experiment; Xianghui Gao performed the transmission electron microscope work and wrote the original draft; Xiyan Zhou performed the pain threshold, analyzed the data and reviewed and edited the manuscript; Hailiang Huang performed the animal experiment and analyzed the data; Yunhua Zang reviewed and edited the manuscript; Li-Wei Chou reviewed and edited the manuscript and provided guidance and advice.

Declaration of conflicting interests

The author(s) declared no potential conflicts of interest with respect to the research, authorship, and/or publication of this article.

Funding

The author(s) disclosed receipt of the following financial support for the research, authorship, and/or publication of this article: This study was funded by Qingdao 2018 medical research guidance plan (Project No: 2018-WJZD031) and Asia University Hospital (11051004).

Data availability

The data that support the findings of this study are available from the corresponding author, upon reasonable request.

ORCID iD

Li-Wei Chou  <https://orcid.org/0000-0002-3540-6225>

References

1. Fu ZH, Wang J, Sun J. Fu's subcutaneous needling: Possible clinical evidence of the subcutaneous connective tissue in acupuncture. *J Altern Complement Med (New York)* 2007; 13: 47–51.
2. Fu ZH. *The Foundation of Fu's Subcutaneous Needling*. Beijing: People's Medical Publishing House, 2016, pp. 116–117.
3. Jia W, Luo L, He LY Systematic review and analysis on the appropriate diseases in clinical treatment with Fu's subcutaneous needling therapy. *Chin Acupuncture* 2019; 39: 111–114.
4. Huang H, Liu J, Fu M Fu's subcutaneous needling for subcutaneous adhesions and scar hyperplasia in the neck region: A case report. *Medicine* 2020; 99: 11–21.
5. Bao X, Wang MH, Liu H Treatment effect and mechanism of Fu's subcutaneous needling among patients with shoulder pain: A retrospective pilot study. *Anatomical Rec (Hoboken, N.J)* 2007; 304: 2552–2558.
6. Fu ZH, Chen XY, Lu LJ Immediate effect of Fu's subcutaneous needling for low back pain. *Chin Med J* 2006; 119: 953–956.

7. Chou LW, Hsieh YL, Kuan TS Needling therapy for myofascial pain: Recommended technique with multiple rapid needle insertion. *Biomedicine* 2014; 4: 1–13.
8. Chiu PE, Fu Z, Jian GW Evaluating effectiveness of fu's subcutaneous needling for the pain nature and quality of life in patients with knee osteoarthritis: A study protocol of randomized clinical trial. *J Pain Res* 2021; 14: 3801–3802.
9. Wang WF. Analysis of the efficacy of differential diagnosis of sciatica and evidence-based treatment of acupuncture. *Chin Ethnic Folk Med* 2012; 21: 83.
10. Qin H. *Meta-analysis of the clinical efficacy of floating needle therapy in lumbar disc herniation*, 11. Liaoning University of Traditional Chinese Medicine, 2017, pp. 22–25.
11. Chou WK. *Clinical Study of Acupuncture for Sciatica Treatment*. Guangzhou University of Traditional Chinese Medicine, 2010, pp. 24–27.
12. Muller FL, Song W, Jang YC Denervation-induced skeletal muscle atrophy is associated with increased mitochondrial ROS production. *Am J Physiol Regul Integr Comp Physiol* 2007; 293: 1159–1168.
13. Sunderland S, Ray -L. Denervation changes in mammalian striated muscle. *J Neurol Neurosurg Psychiatry* 1950; 13: 159–177.
14. Brooks SV, Faulkner -JA. Skeletal muscle weakness in old age: underlying mechanisms. *Med Sci Sports Exerc* 1994; 26: 432–439.
15. Berge OG. Predictive validity of behavioural animal models for chronic pain. *Br J Pharmacol* 2011; 164: 195–1206.
16. Bennet J, Xie YK. A peripheral mononeuropathy in rat that produces disorders of pain sensation like those seen in man. *Pain* 1988; 33: 87–107.
17. Liu ZJ. *Chinese Veterinary Acupuncture and Moxibustion*. China Agricultural Press, 2013, pp. 158–161.
18. Li XD, Huang YY, Yu SN Comparison of mechanical pain thresholds of different positions of Hind Paw in the rat CCI model. *Trop Biol J* 2015; 6: 474–477.
19. Larsen C, Nielisen J, Hansen CN. Biomarkers of mitochondrial content in skeletal muscle of healthy young human subjects. *J Physiol* 2012; 590: 3349–3360.
20. Joffe M, Savage N, Isaacs H. Biochemical functioning of mitochondria in normal and denervated mammalian skeletal muscle. *Muscle Nerve* 1981; 4: 514–519.
21. Adhietty PG, O'Leary MF, Chabi B Effect of denervation on mitochondrially mediated apoptosis in skeletal muscle. *J Appl Physiol* 2007; 10: 1143–1151.
22. Sheu ML, Shen CC, Tsou HK. Dual regeneration of muscle and nerve by intramuscular infusion of mitochondria in a nerve crush injury model. *Pain* 2021; 89: 0–59.
23. Fu Z, Hsieh YL, Hong CZ Remote subcutaneous needling to suppress the irritability of myofascial trigger spots: An experimental study in rabbits. *Evid Based Complement Altern Med* 2012; 2012: 353916.
24. Langevin H, Churchill D, Cipolla M. Mechanical signaling through connective tissue: A mechanism for the therapeutic effect of acupuncture. *Faseb J Official Publ Fed Am Societies Exp Biol* 2001; 15: 82–2275.
25. Yuan L, Bai Y, Yong H. *Conference Proceedings of the 15th Seminar on Regulatory Mechanism of Acupuncture on Body Function and Unique Clinical Experience of Acupuncture and Moxibustion and the 11th Symposium on Acupuncture and Moxibustion 2010*. Anatomical Discover of Meridian and Fascia Theory.
26. Li QY, Huang YX, Peng ZH. Exploring the treatment of neck, shoulder, waist and leg pain based on fascia theory. *External Treat J Traditional Chin Med* 2011; 20: 3–4.
27. Chou JM, Lin YJ, Huang Y. Exploring the mechanism of acupuncture analgesia based on connective tissue. *J Mod Integrated Traditional Chin West Med* 2010; 11: 31–34.
28. Huang CH, Lin CY, Sun MF Efficacy of Fu's subcutaneous needling on myofascial trigger points for lateral epicondylalgia: A randomized control trial. *Evidence-Based Complement Altern Med* 2022; 2022: 5951327.
29. Kimura M, Tohya K, Kuroiwa K. Electron microscopical and immunohistochemical studies on the induction of "qi" employing needling manipulation. *Am J Chin Med* 1992; 20: 25–35.
30. Brand RA. What do tissues and cells know of mechanics? *Ann Med* 1997; 27: 267–269.
31. Tesarz J, Hoheisel U, Wiedenhöfer B. Sensory innervation of the thoracolumbar fascia in rats and humans. *Neuroscience* 2011; 194: 302–308.
32. Stecco C, Pirri C, Fede C. Dermatome and fasciatome. *Clin Anat* 2019; 32: 896–902.
33. Hoheisel U, Rosner J, Mense S. Innervation changes induced by inflammation of the rat thoracolumbar fascia. *Neuroscience* 2015; 300: 351–359.
34. Ni HM, Williams JA, Ding WX. Mitochondrial dynamics and mitochondrial quality control. *Redox Biol* 2015; 4: 6–13.
35. Whitley bn Engelhart-EA-Hoppins- S. Mitochondrial dynamics and their potential as a therapeutic target. *Mitochondrion* 2019; 49: 269–283.
36. Szweczyk A, Wojtczak L. Mitochondria as a pharmacological target. *Pharmacol Rev* 2002; 54: 1–27.
37. Su BD, Xie TQ, Li JW. Understanding the role of mitochondria in the pathogenesis of chronic pain. *Postgrad Med J* 2013; 89: 10–58.
38. Facecchia K, Fochesato LA, Ray SD. Oxidative toxicity in neurodegenerative diseases: role of mitochondrial dysfunction and therapeutic strategies. *J Toxicol* 2011; 12: 683–728.
39. Andreyev Y, Kushnareva Y.E, Starkov AA. Mitochondrial metabolism of reactive oxygen species. *Biochemistry* 2005; 70: 200–214.
40. Lee I, Kim HK, Kim JH. The role of reactive oxygen species in capsaicin-induced mechanical hyperalgesia and in the activities of dorsal horn neurons. *Pain* 2007; 133: 9–17.

41. Napolitano G, Fasciolo G, Venditti P. *Mitochondrial Management of Reactive Oxygen Species*, 10. Basel, Switzerland: Antioxidants, 2021.
42. Valko M, Rhodes C, Moncol J. Free radicals, metals and antioxidants in oxidative stress-induced cancer. *Chem Biol* 2020; 160: 1–40.
43. Zorov DB, Juhaszova M, Sollott SJ. Mitochondrial reactive oxygen species (ROS) and ROS-induced ROS release. *Physiol Rev* 2014; 94: 909–950.
44. Wacquier B, Combettes L, Dupont G. Dual dynamics of mitochondrial permeability transition pore opening. *Scientific Rep* 2020; 10: 3924.
45. Zaib S, Hayyat A, Ali N. Role of mitochondrial membrane potential and lactate dehydrogenase a in apoptosis. *Anti-cancer Agents Med Chem* 2021: 21.
46. Lee C, Tian R. Mitochondrion as a target for heart failure therapy- role of protein lysine acetylation. *Circ J Official J Jpn Circ Soc* 2015; 79: 70–1863.